

Contents lists available at [ScienceDirect](https://www.sciencedirect.com)

# Ecological Complexity

journal homepage: [www.elsevier.com/locate/ecocom](https://www.elsevier.com/locate/ecocom)

Original research article



## Integrals of life: Tracking ecosystem spatial heterogeneity from space through the area under the curve of the parametric Rao's Q index

Elisa Thouverai<sup>a,\*</sup>, Matteo Marcantonio<sup>b,1</sup>, Jonathan Lenoir<sup>c</sup>, Mariasole Galfré<sup>a</sup>,  
 Elisa Marchetto<sup>a</sup>, Giovanni Bacaro<sup>d</sup>, Roberto Cazzolla Gatti<sup>a</sup>, Daniele Da Re<sup>b</sup>,  
 Michele Di Musciano<sup>a,e</sup>, Reinhard Furrer<sup>f</sup>, Marco Malavasi<sup>g</sup>, Vítězslav Moudrý<sup>h</sup>,  
 Jakub Nowosad<sup>i</sup>, Franco Pedrotti<sup>j</sup>, Raffaele Pelorosso<sup>k</sup>, Giovanna Pezzi<sup>a</sup>, Petra Šímová<sup>g</sup>,  
 Carlo Ricotta<sup>l</sup>, Sonia Silvestri<sup>m</sup>, Enrico Tordoni<sup>n</sup>, Michele Torresani<sup>o</sup>, Giorgio Vacchiano<sup>p</sup>,  
 Piero Zannini<sup>a,q,r</sup>, Duccio Rocchini<sup>a,g</sup>

<sup>a</sup> BIOME Lab, Department of Biological, Geological and Environmental Sciences, Alma Mater Studiorum University of Bologna, via Irnerio 42, 40126 Bologna, Italy

<sup>b</sup> Evolutionary Ecology and Genetics Group, Earth & Life Institute, UCLouvain, 1348 Louvain-la-Neuve, Belgium

<sup>c</sup> UMR CNRS 7058, Ecologie et Dynamique des Systèmes Anthropisés (EDYSAN), Université de Picardie Jules Verne, 1 rue des Lovelux, F-80037 Amiens Cedex 1, France

<sup>d</sup> Department of Life Sciences, University of Trieste, via Giorgieri 10, 34127 Trieste, Italy

<sup>e</sup> Department of Life, Health and Environmental Sciences, University of L'Aquila, Piazzale Salvatore Tommasi 1, 67100, L'Aquila, Italy

<sup>f</sup> Department of Mathematics and Institute of Computational Science, University of Zürich, Zürich, Switzerland

<sup>g</sup> Department of Chemistry, Physics, Mathematics and Natural Sciences, University of Sassari, Sassari, Italy

<sup>h</sup> Department of Spatial Sciences, Faculty of Environmental Sciences, Czech University of Life Sciences Prague, Praha - Suchbátka, Czech Republic

<sup>i</sup> Institute of Geocology and Geoinformation, Adam Mickiewicz University, Krygowskiego 10, 61-680 Poznań, Poland

<sup>j</sup> University of Camerino, Camerino, Italy

<sup>k</sup> DAFNE Department, Tuscia University, 01100 Viterbo, Italy

<sup>l</sup> Department of Environmental Biology, Sapienza University, Piazzale Moro, 5, 00185, Rome, Italy

<sup>m</sup> Department of Biological, Geological and Environmental Sciences, Alma Mater Studiorum University of Bologna, via Irnerio 42, 40126 Bologna, Italy

<sup>n</sup> Department of Botany, Institute of Ecology and Earth Sciences, University of Tartu, J. Liivi 2, 50409 Tartu, Estonia

<sup>o</sup> Libera Università di Bolzano - Freie Universität Bozen, Bolzano/Bozen, Italy

<sup>p</sup> Department of Agricultural and Environmental Sciences (DiSAA), Università degli Studi di Milano, Via Celoria 2, 20133 Milano, Italy

<sup>q</sup> LifeWatch Italy, Lecce

<sup>r</sup> Plant Data – Interuniversity Research Centre for Plant Biodiversity and Big Data, Department of Biological, Geological and Environmental Sciences, University of Bologna, Bologna, Italy

### ARTICLE INFO

**Keywords:**  
 Biodiversity  
 Ecological informatics  
 Modelling  
 Remote sensing  
 Satellite imagery

### ABSTRACT

Spatio-ecological heterogeneity is strongly linked to many ecological processes and functions such as plant species diversity patterns and change, metapopulation dynamics, and gene flow. Remote sensing is particularly useful for measuring spatial heterogeneity of ecosystems over wide regions with repeated measurements in space and time. Besides, developing free and open source algorithms for ecological modelling from space is vital to allow to prove workflows of analysis reproducible. From this point of view, NASA developed programs like the Surface Biology and Geology (SBG) to support the development of algorithms for exploiting spaceborne remotely sensed data to provide a relatively fast but accurate estimate of ecological properties in vast areas over time. Most of the indices to measure heterogeneity from space are point descriptors: they catch only part of the whole heterogeneity spectrum. Under the SBG umbrella, in this paper we provide a new R function part of the rasterdiv R package which allows to calculate spatio-ecological heterogeneity and its variation over time by considering all its possible facets. The new function was tested on two different case studies, on multi- and hyperspectral images, proving to be an effective tool to measure heterogeneity and detect its changes over time.

\* Corresponding author.

E-mail address: [elisa.thouverai2@unibo.it](mailto:elisa.thouverai2@unibo.it) (E. Thouverai).

<sup>1</sup> Authors equally contributed to the manuscript.

<https://doi.org/10.1016/j.ecocom.2023.101029>

Received 30 September 2022; Accepted 31 January 2023

Available online 14 February 2023

1476-945X/© 2023 The Authors. Published by Elsevier B.V. This is an open access article under the CC BY-NC-ND license (<http://creativecommons.org/licenses/by-nc-nd/4.0/>).

## 1. Introduction

The concept of spatiotemporal heterogeneity is crucial in ecological modelling to link spatial patterns to the generating processes and to the functional networking among organisms (Borcard et al., 1992). In ecological research, the search for new methods underlying spatiotemporal patterns in ecosystem heterogeneity has been a recurring theme (Rocchini and Ricotta, 2007; Atluri et al., 2018). Spatio-ecological heterogeneity, in this paper considered as the degree of non-uniformity in vegetation, land cover, and physical factors (soil, topography, microclimate and topoclimate; Stein et al. (2014)), has been proven to be strongly linked to many ecological processes and functions such as plant species diversity patterns and change (Rocchini et al., 2018), metapopulation dynamics (Fahrig, 2007), and gene flow (Lozier et al., 2013). Indeed, an increase of spatial heterogeneity means an increase in the availability of ecological niches, provision of refuges at relatively short distances and opportunities for spatial isolation and local adaptation (Stein et al., 2014). As a consequence, species coexistence, persistence and diversification are generally in strict relation with the degree of environmental heterogeneity available within the landscape (Stein et al., 2014; Tews et al., 2004). The development of new methods for measuring spatio-ecological heterogeneity is also fundamental to make estimations of its change in time in order to improve conservation planning (Skidmore et al., 2021).

In this context, NASA developed programs like the Global Ecosystem Dynamics Investigation (GEDI, <https://gedi.umd.edu/>) or the Surface Biology and Geology (SBG) mission (<https://science.nasa.gov/earth-science/decadal-sbg>) exploiting spaceborne remotely sensed data to provide a relatively fast but accurate estimate of spatio-ecological heterogeneity in vast areas over time. In fact, spectral heterogeneity of an optical image – associated with the reflectance values of the pixels – can be a proxy of the spatio-ecological heterogeneity (Rocchini, 2007). Hence, the variation of spatio-ecological heterogeneity in space and time (e.g., phenological cycles) can be effectively inferred using remote sensing (Schneider et al., 2017).

Therefore, the measure of ecosystem heterogeneity over time from satellite through Free and Open Source Software and algorithms allows robust, reproducible and standardized estimates of ecosystem patterns and processes (Rocchini and Neteler, 2012). Also, its use brings many advantages: availability, transparency and shareability. In this context, the R platform is one of the most used statistical and computational environment in ecology, partially thanks to the continuous development of relevant packages. In particular, the `rasterdiv` package (Marcantonio et al., 2021; Rocchini et al., 2021b; Thouverai et al., 2021) allows to calculate a plethora of different indices to measure spatio-ecological heterogeneity from space.

Most of the algorithms have been related to Information Theory relying on abundance-based metrics, starting from Shannon's index (Simpson, 1949) (see Section 2). However, some information about the spectral distance among pixel reflectance values might be lost if not considered in the calculation (Rocchini et al., 2017). Currently, the candidate for solving the problem is Rao's Quadratic Entropy index (hereafter Rao's Q) (Rao, 1982): this index, besides the relative abundance of pixel values in a given moving window or polygonal area, incorporates also their spectral distances (Section 2). Both Shannon and Rao's Q indices are point descriptors of heterogeneity, namely they can only show part of the whole heterogeneity spectrum. Recently Rocchini et al. (2021a) proposed an implementation of the Rao's Q index by parameterizing the original formula, and allowing the whole continuum of heterogeneity to be measured thanks to Rao's Q continuous profiles (see Section 2).

This paper aims to show how to make proper use of the Rao's continuum heterogeneity variation profile by proposing a new R function – integrated into the `rasterdiv` R package (Marcantonio et al., 2021) – which calculates AUC, the area under the curve formed by applying the parametric Rao's Q index (see Section 2). Two case studies on multi- and hyperspectral satellite images are also provided in order to verify if the new metric proposed could be an effective tool for the study of spatio-ecological heterogeneity.

## 2. The algorithm

### 2.1. The theory

Algorithms that aim to measure environmental heterogeneity through remote sensing data can rely on the moving window technique, which divides remotely sensed imagery into user-defined squares (windows) to derive measures of heterogeneity. Examples are included in the `rasterdiv` R package (Rocchini et al., 2021b). One of the most used metrics included in the package is the Shannon entropy index  $H$  (Shannon, 1948):

$$H = - \sum_{i=1}^N p_i \ln p_i \quad (1)$$

where the relative abundance of every pixel reflectance value calculated as the ratio between the actual value of the pixel  $i \in \{1, \dots, N\}$  and the sum of the pixel values of the moving window ( $p_i$ ) in an image of  $N$  pixels is considered. It is usually calculated of one layer images, such as a vegetation index or the first axis of a PCA. However, Shannon's  $H$  does not consider the spectral distances among pixel reflectance values, overestimating the heterogeneity of homogeneous surfaces (Rocchini et al., 2017). For instance, when using Shannon's  $H$ , spectral values differing by a few decimals will be treated the same as spectral values differing by several order of magnitudes. To overcome this issue, Rao's Q index (Rao, 1982) can be used to include the pixel's spectral distances in the calculation:

$$Q = \sum_{i=1}^N \sum_{j=1}^N d_{ij} \times p_i \times p_j \quad (2)$$

where  $d_{ij}$  is the spectral distance between pixel  $i$  and pixel  $j$  and  $p_i$  and  $p_j$  are the relative abundances of the pixels  $i$  and  $j$  in an assemblage of  $N$  pixels. The spectral distance between pixels  $d_{ij}$  can be calculated over any number of layers and using any metric for the calculation of pairwise distances. For example, in the `rasterdiv` package, the Rao function permits the calculation of Rao's Q choosing from "euclidean", "manhattan", "canberra", "minkowski" and "mahalanobis" as the type of distance calculated (Marcantonio et al., 2021). Both Shannon's  $H$  and Rao's Q are point descriptors of heterogeneity, showing only one part of its potential spectrum. Therefore, the use of generalized entropies, where one single formula represents a parameterized version of an index, provides a continuum of heterogeneity metrics reflecting all the characteristics of the heterogeneity spectrum. Rocchini et al. (2021b) presented a parametric version of Rao's Q allowing the characterization of the dimensionality of heterogeneity in different ecosystems:

$$Q_\alpha = \left( \sum_{i,j=1}^N \omega_{ij} d_{ij}^\alpha \right)^{\frac{1}{\alpha}} \quad (3)$$

where  $d_{ij}$  is the spectral distance between pixel  $i$  and pixel  $j$  and  $\omega_{ij}$  is the combined probability ( $1/N^2$ ) of extracting pixels  $i$  and  $j$  in this order in an image of  $N$  pixels. In other words, parametric Rao's Q is a generalized mean that measures the expected distance between two randomly chosen pixels regulated by the parameter  $\alpha$ . The  $\alpha$  parameter provides a continuum of potential diversity indices by regulating the weight of  $d_{ij}$  with the highest values obtaining different types of means as it is increasing ( $[\alpha \rightarrow 0] \Rightarrow$  geometric,  $[\alpha = 1] \Rightarrow$  arithmetic,  $[\alpha = 2] \Rightarrow$  quadratic,  $[\alpha = 3] \Rightarrow$  cubic, and so on till  $[\alpha \rightarrow \infty] \Rightarrow \max_d$ ).

In this paper, we propose to calculate the area under the curve (AUC) constructed by applying the index parametric Rao's Q over a sequence of  $\alpha$  values. We want to verify if AUC can be used to quantify the width of the diversity spectrum calculated with parametric Q for each pixel, resulting in an image that can be exploited to monitor the change in the heterogeneity spectrum over time for a selected area.

### 2.2. The R function

The function `rasterdiv::RaoAUC()` exploits the function `rasterdiv::paRao()` to define the values of the parametric Rao's Q

using a vector of alphas decided by the user. Accordingly, the values of parametric Rao's Q are calculated building a moving window around every pixel of the remote sensing image for every alpha selected. Then, the integral of the curve formed by the values of the parametric Rao's Q index obtained for every pixel is calculated.

### 3. Examples

In this section, we present one theoretical examples and two case studies for the new R function proposed (RaoAUC()). Specifically, AUC was calculated for one layer, multi- and hyperspectral satellite images of areas afflicted by a sudden event that changed the spatio-ecological heterogeneity of the area. We choose two images per case study of two different moments in time and calculated the difference between the two, highlighting the increase in heterogeneity.

#### 3.1. A theoretical example

In this section, we will show how to use the function accRao() from the rasterdiv package to calculate the accumulation function (integral) of Rao values obtained using a range of alpha-values. We used a raster for the global average NDVI rescaled at 8-bit available from rasterdiv. This raster was first cropped on the islands of Sardinia and Corsica. In order to simulate the effects of an ecological perturbation, for example widespread drought, we created a new raster with perturbed NDVI values for these two islands. Pixels with NDVI higher than 150 were decreased using values from a normal distribution centred on 50 with a standard deviation of 5. Then, we applied accRao() both on the original and simulated raster by using alphas ranging from 1 to 10:

```
RaoAUC.before ← accRao(
  alphas = 1:10, #range of alphas

  x = ndvi.before, #raster layer

  dist_m = "euclidean", #method for the
                        #calculation of the
                        #spectral distance

  window = 3, #dimension of the moving window

  method = "classic", #specifies if the function
                    #is applied on a single
                    #layer or on a
                    #multidimensional system

  rasterAUC = TRUE, #specifies if the output
                  #will be a raster layer or
                  #a matrix

  na.tolerance = 0.4, #proportion of NA values
                    #tolerated

  np = 1 #number of cores which will be spawned
)

RaoAUC.after ← accRao(
  alphas = 1:10,
  x = ndvi.after,
  dist_m = "euclidean",
  window = 3,
  method = "classic",
  rasterAUC = TRUE,
  na.tolerance = 0.4, np = 1)
```

Afterwards, the difference between the two rasters, before and after the simulated perturbation, was calculated (Fig. 1). Also, the average parametric Rao of the images in Fig. 1 was calculated for every  $\alpha$  value, and the resulting curves are showed in Fig. 2.

accRao() function derives the value of parametric Rao for each pixel using a moving window algorithm. To illustrate how this methodology works, we applied paRao() on a single group of neighbour pixels, which represents a moving window, from the two NDVI rasters and with alphas ranging from 1 to 10 as follows:

```
#Selection of the 3x3 window
ndvi.pix.b ← ndvi.before[41:43, 21:23,drop=FALSE]
ndvi.pix.a ← ndvi.after[41:43, 21:23,drop=FALSE]

#Set the alpha interval
alphas ← 1:10

#Set the number of pixels in the selected window
N ← 3^2

#Function to calculate paRao over the set alphas
RaoFx ← function(alpha,N,D) {
  ( sum((1/(N^4)) * D^alpha ) * 2)^(1/alpha)
}

#Calculation of paRao before
rao.b ← sapply(alphas, function(a) {
  RaoFx(alpha = a, N = N,D = as.vector(ndvi.pix.b))})

#Calculation of paRao after
rao.a ← sapply(alphas, function(a) {
  RaoFx(alpha = a, N = N,
  D = as.vector(ndvi.pix.a))})
```

From the values obtained (a parametric value for each alpha), the area under the curve was calculated integrating the results (Fig. 3):

```
#Calculation of AUC before
RaoAUC.bf ← approxfun(x = alphas, y = rao.b)
RaoAUC.b ← integrate(RaoAUC.bf, lower = 1,
  upper = 10, subdivisions = 500)

#Calculation of AUC after
RaoAUC.af ← approxfun(x = alphas, y = rao.a)
RaoAUC.a ← integrate(RaoAUC.af, lower = 1,
  upper = 10, subdivisions = 500)
```

#### 3.2. Empirical examples

In this section, the accRao() function is tested on two real-world case studies by comparing remotely sensed images before and after a perturbation event. AUC is calculated on multi- and hyperspectral images, exploiting the information that every band holds to estimate the spatio-ecological heterogeneity.

##### 3.2.1. Example 1: Fire spread in the Kangaroo island (Australia)

This section focuses on the major fire-affected area of Kangaroo Island in January 2020, in particular on Flinders Chase NP and the associated Ravine Des Casoars Wilderness Protection Area. Two cloudless images from Copernicus Sentinel-2 (<https://sentinels.copernicus.eu/web/sentinel/missions/sentinel-2>) with a spatial resolution of 10 m before (January 2019) and after (January 2021) were compared (Fig. 4).

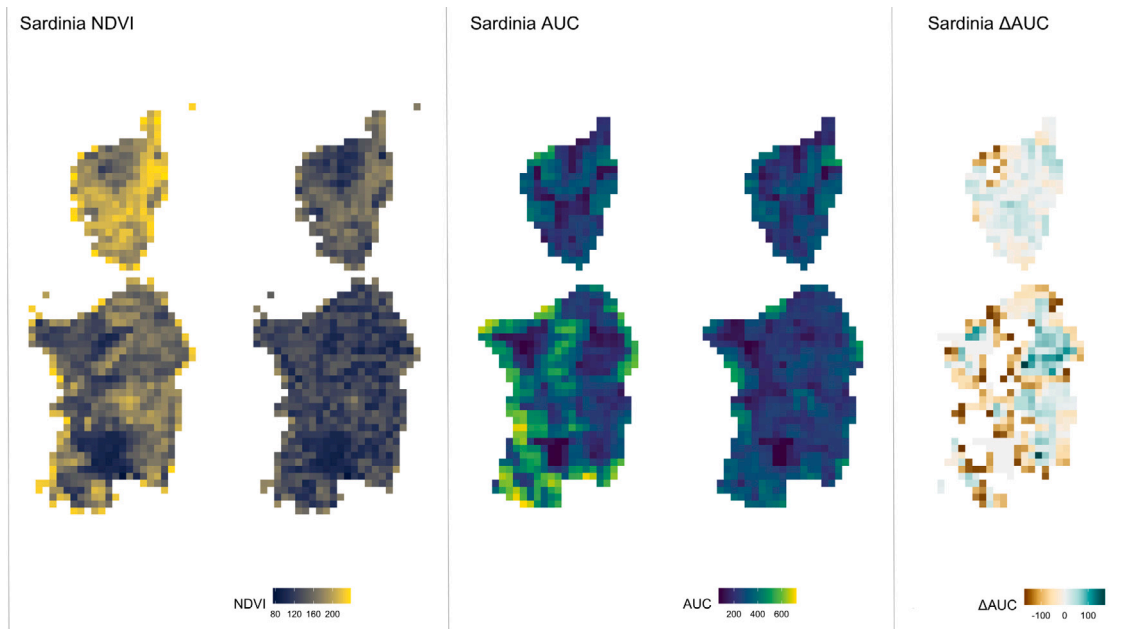


Fig. 1. From left to right: the NDVI images of Sardinia and Corsica before and after the simulated perturbation, the correspondent AUC images and their difference after — before the simulated perturbation.

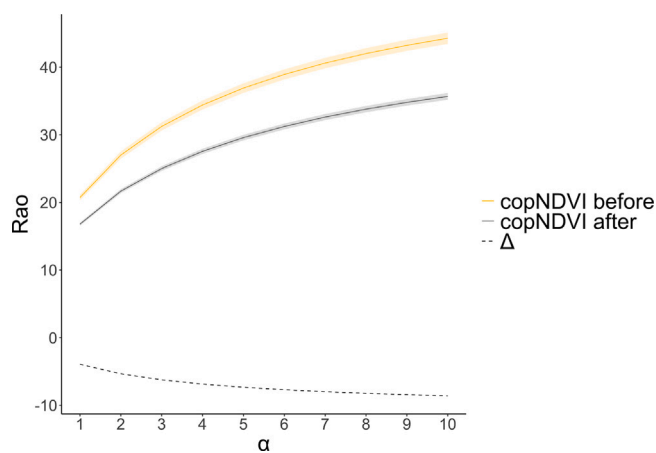


Fig. 2. Three curves representing respectively: the mean values of parametric Rao's Q (i) before (yellow) and (ii) after (grey) the simulated ecological perturbation (drought) of Fig. 1, their correspondent confidence intervals and (iii) their difference (after-before, dashed line) over increasing alphas.

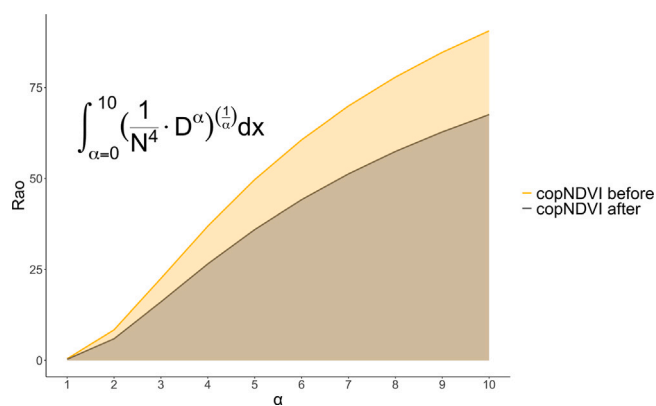


Fig. 3. Curves representing the values of parametric Rao's Q for one pixel before (yellow) and after (grey) the simulated ecological perturbation (drought) of Fig. 1 over increasing alphas. The area under the curve (AUC) is highlighted.

The `accRao()` function was applied on the 2 multispectral images (Red, Green, Blue and NIR bands) using a moving window of  $9 \times 9$  pixels and the parameter alpha was set to a range of 1 to 5:

```
#accRao() function
accRao(alphas = 1:5, x = kanga_multi,
       dist_m = "euclidean", window = 9,
       method = "multidimension", rasterAUC = TRUE,
       na.tolerance = 0.9, np = 1)
```

Subsequently, the difference between the obtained AUC images was calculated, with positive values meaning an increase in spatio-ecological heterogeneity (Fig. 4). In this case, the AUC of Rao's Q profiles succeeded to highlight areas where the perturbation (fire) event caused an increase of spatial heterogeneity of vegetation which was more homogeneous (continuous woodland cover) before the perturbation.

### 3.2.2. Example 2: Post fire in Santa Barbara, California

For the last empirical examples two hyperspectral images of a post-fire scene in Santa Barbara (California) were downloaded from AVIRIS <https://aviris.jpl.nasa.gov/> platform. The first image is from June 2009, the second from June 2011 in order to visualize the recovery of the vegetation after the fire event (see Fig. 5). The `accRao()` function was applied over all the 224 bands of the two images using a moving window of  $9 \times 9$  pixels and setting the  $\alpha$  parameter to a range of one to 5:

```
#accRao() function
accRao(alphas = 1:5, x = santabarbara_hyper,
       dist_m = "euclidean", window = 9,
       method = "multidimension", rasterAUC = TRUE,
       na.tolerance = 0.9, np = 1)
```

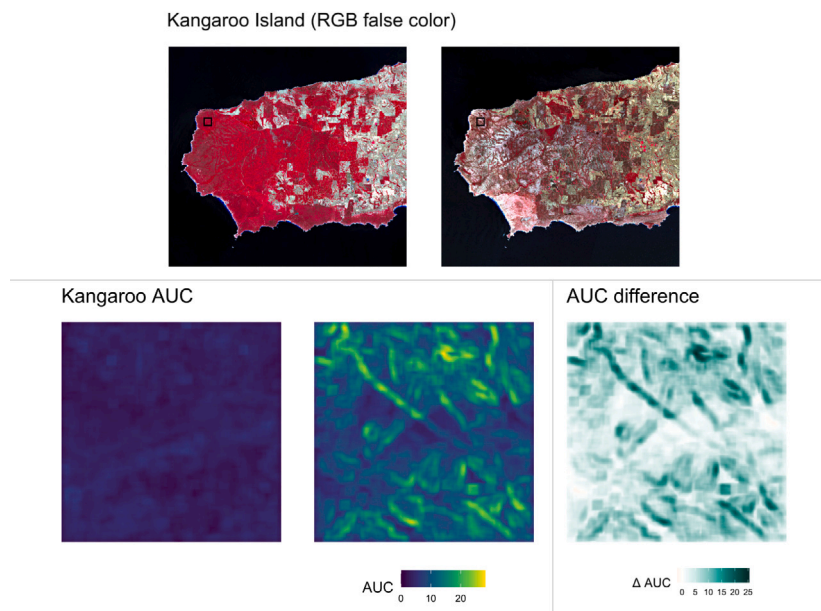


**Fig. 4.** On top, the Kangaroo Island before and after the fires (the area used for the analysis is highlighted) and the selected area before and after the fire in RGB false colour (NIR, red, green); on the bottom the correspondent AUC images and their difference after-before the fire.

Subsequently, the difference between the obtained AUC images was calculated as in the previous examples (Fig. 6). The difference between the obtained AUC highlights subtle changes of spatio-ecological heterogeneity in the studied area between 2009 and 2011.

#### 4. Discussion

The study of landscape structure has been steadily growing in recent years (e.g., Lichstein et al., 2002; Saravia, 2015; Marcantonio et al., 2013) with the development of several methodologies and approaches, which have been tested ecosystems and supported in the scientific literature (see Bar-Massada and Wood, 2014). In particular, the use and availability of remote sensing data have made it possible to assess specific heterogeneity patterns over various ecosystems, with increasing performance in terms of spectral/spatial/temporal characteristics, opening up new possibilities for exploring complex ecological processes.

Using our algorithm, environmental heterogeneity is estimated by the range of spectral values associated to the spatial variability within a given habitat. Hence, environmental heterogeneity can be evaluated contiguously, from regional to continental extents, according to the remote sensing data used and the spatial extent of the analysis. Among the heterogeneity metrics, parametric Rao's Q adds a layer of information to classical estimates of heterogeneity from remotely sensed multispectral data. This index considers pairwise pixel spectral distance to separate areas with high richness but low evenness from those with low richness but high evenness (Rocchini et al., 2017).

In addition, the parametric Rao's Q can be calculated in a multivariate system such as a multi-temporal system, i.e. long time series, in order to improve the assessments and prediction of changes in spatio-ecological heterogeneity over space and time (Rugani and Rocchini, 2016). Also, by considering multiple bands, it has a higher capability to discern subtle diversity changes over the landscape (Torresani et al., 2019).

In this paper, all the potential facets of heterogeneity were investigated by parameterizing the Rao's Q metric and calculating the area under the curve of continuous entropy profiles. This would be particularly useful when dealing with multitemporal sets, with increases or decreases of heterogeneity provoked by different ecological

processes like drought (Section 3.1, see also Jiao et al., 2020) and fire (Section 3.2.1, see also Chuvieco and Kasischke, 2007; Section 3.2.2).

The application of AUC on Rao's Q in before/after ecological perturbation scenarios can help pointing out areas with the highest difference in spectral heterogeneity, by considering the whole heterogeneity continuum. For example, Section 3.2.2 of two postfire scenes shows the sensibility of the algorithm in highlight even subtle landscape changes using multiple bands for the analysis. Heterogeneity of ecosystems is multifaceted in its very nature. As stressed by Gorelick (2011) there is no "true heterogeneity" measurement since important holistic aspects of ecosystems are inevitably lost once making use of single metrics. From this point of view, the proposed generalized entropy, based on a parameterization of the Rao's Q entropy (and its area under the curve) can help catching the multidimensionality of ecosystem heterogeneity components (Nakamura et al., 2020), avoiding the intrinsic fallacy of a single best index of true heterogeneity (Gorelick, 2011).

Moreover, the Rao's Q original formula directly takes into account the distance among values (pixel reflectances once applied to remote sensing imagery). This leads to the possibility of accounting for the turnover among reflectances, also known as beta-diversity in ecology (Rocchini et al., 2018). Since little consensus has been reached as to general measures of heterogeneity/beta-diversity measurement in literature (Koleff et al., 2003), the aforementioned use of a generalized metric like the parametric Rao's Q helps detecting gradients in reflectance beta-diversity change (turnover) over space, otherwise hidden when relying on point descriptors of heterogeneity, i.e. single metrics like the commonly used Shannon and Simpson indices in remote sensing applications (Nagendra, 2002). In other words, while a wide range of approaches has been used to catch the variation of ecosystem properties, finding ways to generalize heterogeneity measurement could represent a consistent approach to describe heterogeneity patterns change in space and time (Haralick and Kelly, 1969).

The use of a continuum of diversities as in the parametric Rao's Q leads to the understanding of hidden parts of the whole diversity of dimensionalities (Nakamura et al., 2020). Increasing alpha in Eq. (3) will increase the weight of higher distances among different values until reaching the maximum distance value possible (Rocchini et al., 2021a). For this reason, spatio-ecological heterogeneity values of the parametric Rao's Q increase with each alpha progressively added to the calculation constructing a curve for every moving window built around

## Santa Barbara RGB



Fig. 5. Post fire in Santa Barbara 2009 (left) and 2011 (right). The area within the square is the studied area.

each pixel (Rocchini et al., 2021b). Consequently, applying an integral, it is possible to calculate the area under every pixel's window area curve obtaining a new spatio-ecological heterogeneity metric, AUC. Hence, the  $\text{accRao}()$  function can highlight the differences before and after an ecological perturbation both in the theoretical and in the empirical examples (Figs. 1, 4 and 6) showing the change in the whole heterogeneity continuum and being able to detect both: (i) spatially wide heterogeneity change patterns, as in the Kangaroo Island's fires example (see Section 3.2.1), as well as (ii) spatially localized differences

in space and time, as in the post fire in Santa Barbara example (see Section 3.2.2).

The three examples proposed in Section 3, show the application of AUC on one layer (Section 3.1), multispectral (Section 3.2.1) and hyperspectral (Section 3.2.2) satellite images. However, for the hyperspectral images it is difficult to address a cause for the heterogeneity change: because of the high number of bands exploited for the analysis we cannot know which ones weight more in the measure of the index. Analysis like the Principal Component Analysis (PCA) or correlation matrices can help to highlight the bands which give more contribution in the calculation of the spatio-ecological heterogeneity.

Also, in the empirical case studies only a range of alpha between 1 and 5 was tested because of the high computational complexity of the function  $\text{accRao}()$  as it is now. We are actually working to speed up the algorithm, so it would be interesting in a future study to test different ranges of alpha. In this context, it would also be helpful the study of the influence of the number of bands and their resolution on the measure of AUC, as highlighted by the Santa Barbara subsection (see Section 3.2.2).

In conclusion, the integration over an alpha range is more convenient than having to choose a single alpha level as the most representative level of diversity. This task is often complicated as there is no direct interpretation for the meaning of indices calculated with different alphas. Here, we propose the way forward to re-conciliate the advantage of having a single metrics without the need of choosing a single alpha value.

## 5. Conclusion

In this paper, we provided a practical demonstration of the effectiveness of a method that can supply measures of generalized entropy at different spatial scales and in different contexts. Generalized means represent an effective tool to develop a unifying notation for a large family of parametric diversity and dissimilarity functions (Ricotta et al., 2021). Indeed, binding different heterogeneity metrics in order to analyse ecosystem changes proved to be a reliable approach to enhance the output information. Although remote sensing data have long held the promise of transforming environmental monitoring efforts, publicly accessible tools leveraging these data to achieve actionable in-sights have been lacking. We suggest that Rao's AUC can be useful to identify areas more vulnerable to environmental changes, and to develop and implement appropriate habitat management plans and environmental policies.

## Declaration of competing interest

The authors declare that they have no known competing financial interests or personal relationships that could have appeared to influence the work reported in this paper.

## Data availability

The code and the data used are opensource and available online.

## Acknowledgements

This study has received funding from the project SHOWCASE (SHOW-CASingsynergies between agriculture, biodiversity and ecosystems services to help farmers capitalising on native biodiversity) within the European Union's Horizon 2020 Researcher and Innovation Programme under grant agreement No. 862480. DR was also supported by the Horizon Europe project Earthbridge.

PZ was supported by LifeWatch Italy through the project LifeWatch-PLUS (CIR01\_00028).

RF is supported by the Swiss National Science Foundation, Switzerland SNSF175529.

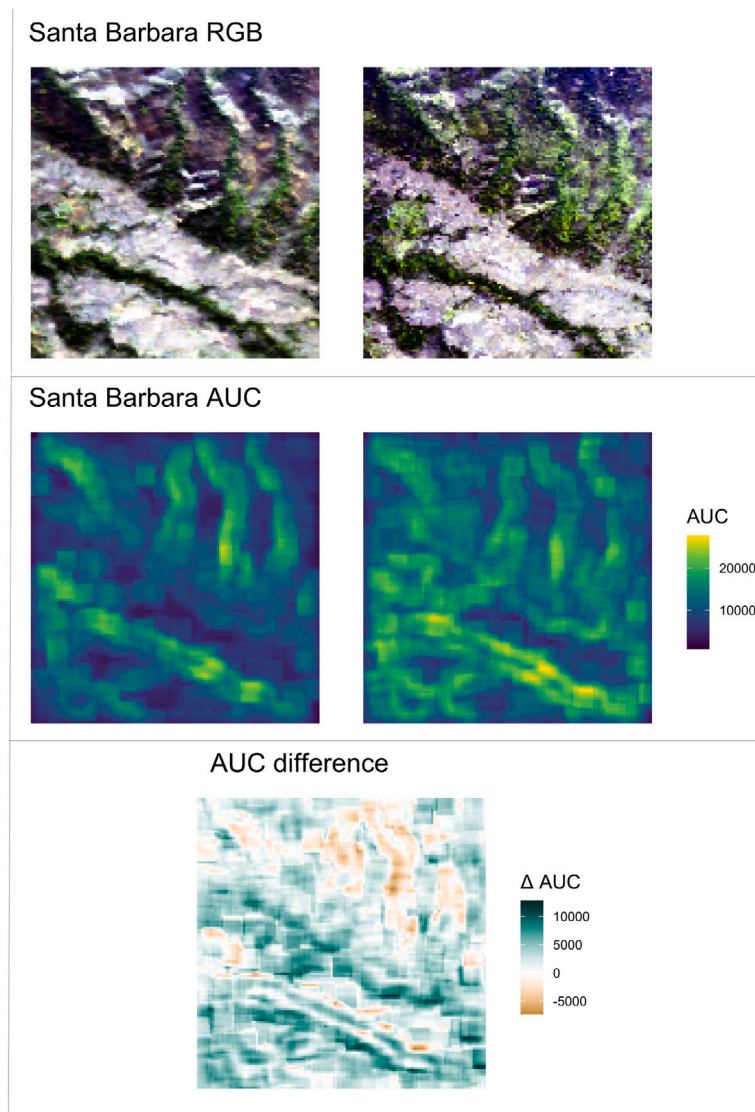


Fig. 6. From the top: RGB images of the study area (Santa Barbara, CA) in 2009 and 2011, the correspondent AUC images and their difference 2011–2009.

ETo is supported by the Estonian Research Council, grant code MOBJD1030.

MM is supported by the FRS-FNRS and by the “Action de Recherche concertée” grant number 17/22-086.

DR, MM, MG and ETH contributed to the development of the R function and to the analysis. DR, PZ and ETH contributed to the implementation of the figures. All the authors contributed to the writing of the manuscript.

The rasterdiv package that contains the new function proposed can be downloaded at <https://github.com/mattmar/rasterdiv> or directly from the CRAN (<https://CRAN.R-project.org/package=rasterdiv>). The hyperspectral images of Santa Barbara of June 2009 and 2011 can be respectively retrieved from [https://popo.jpl.nasa.gov/avcl/y09\\_data/f090826t01p00r08.tar.gz](https://popo.jpl.nasa.gov/avcl/y09_data/f090826t01p00r08.tar.gz) and [https://popo.jpl.nasa.gov/avcl/y11\\_data/f110719t01p00r19.tar.gz](https://popo.jpl.nasa.gov/avcl/y11_data/f110719t01p00r19.tar.gz). The images of Kangaroo Island can be retrieved from <https://scihub.copernicus.eu/dhus/#/home>.

## References

- Atluri, G., Karpatne, A., Kumar, V., 2018. Spatio-temporal data mining: A survey of problems and methods. *ACM Comput. Surv.* 51, 4–45.
- Bar-Massada, A., Wood, E.M., 2014. The richness-heterogeneity relationship differs between heterogeneity measures within and among habitats. *Ecography* 37, 1–8.
- Borcard, D., Legendre, P., Drapeau, P., 1992. Partialling out the spatial component of ecological variation. *Ecology* 73, 1045–1055.
- Chuvieco, E., Kasischke, E.S., 2007. Remote sensing information for fire management and fire effects assessment. *J. Geophys. Res.: Biogeosci.* 112, G01S90.
- Fahrig, L., 2007. Landscape heterogeneity and metapopulation dynamics. In: Wu, J., Hobbs, R. (Eds.), *Key Topics in Landscape Ecology*. Cambridge University Press, Cambridge, UK, pp. 78–91.
- Gorelick, R., 2011. Commentary: Do we have a consistent terminology for species diversity? The fallacy of true diversity. *Oecologia* 167, 885–888.
- Haralick, R.M., Kelly, G.L., 1969. Pattern recognition with measurement space and spatial clustering for multiple images. *Proc. IEEE* 57 (4), 654–665.
- Jiao, T., Williams, C.A., Rogan, J., De Kauwe, M.G., Medlyn, B.E., 2020. Drought impacts on Australian vegetation during the millennium drought measured with multisource spaceborne remote sensing. *J. Geophys. Res.: Biogeosci.* 125, e2019JG005145.
- Koleff, P., Gaston, K.J., Lennon, J.J., 2003. Measuring beta diversity for presence-absence data. *J. Anim. Ecol.* 72, 367–382.
- Lichstein, J.W., Simons, T.R., Shriver, S.A., Franzreb, K.E., 2002. Spatial autocorrelation and autoregressive models in ecology. *Ecol. Monograph* 72, 445–463.
- Lozier, J.D., Strange, J.P., Koch, J.B., 2013. Landscape heterogeneity predicts gene flow in a widespread polymorphic bumble bee, *Bombus Bifarius* (Hymenoptera: Apidae). *Conserv. Genet.* 14, 1099–1110.
- Marcantonio, M., Iannacito, M., Thouverai, E., Da Re, D., Tattoni, C., Bacaro, G., Vicario, S., Ricotta, C., Rocchini, D., 2021. rasterdiv: Diversity indices for numerical matrices. R package version 0.2-3. <https://CRAN.R-project.org/package=rasterdiv>.
- Marcantonio, M., Rocchini, D., Geri, F., Bacaro, G., Amici, V., 2013. Biodiversity, roads, & landscape fragmentation: two mediterranean cases. *Applied Geography* 42, 63–72.

- Nagendra, H., 2002. Opposite trends in response for the Shannon and Simpson indices of landscape diversity. *Appl. Geogr.* 22, 175–186.
- Nakamura, G., Gon calves, L.O., Duarte, L.d.S., 2020. Revisiting the dimensionality of biological diversity. *Ecography* 43, 539–548.
- Rao, C.R., 1982. Diversity and dissimilarity coefficients: A unified approach. *Theor. Popul. Biol.* 21, 24–43.
- Ricotta, C., Szeidl, L., Pavoine, S., 2021. Towards a unifying framework for diversity and dissimilarity coefficients. *Ecol. Indic.* 129, 107971.
- Rocchini, D., 2007. Effects of spatial and spectral resolution in estimating ecosystem alpha-diversity by satellite imagery. *Remote Sens. Environ.* 111, 423–434.
- Rocchini, D., Luque, S., Pettorelli, N., Bastin, L., Doktor, D., Faedi, N., et al., 2018. Measuring beta-diversity by remote sensing: A challenge for biodiversity monitoring. *Methods Ecol. Evol.* 9, 1787–1798.
- Rocchini, D., Marcantonio, M., Re, D.Da., Bacaro, G., Feoli, E., Foody, G.M., et al., 2021a. From zero to infinity: Minimum to maximum diversity of the planet by spatio-parametric Rao's quadratic entropy, global ecology and biogeography. *Global Ecol. Biogeogr.* 30, 1153–1162.
- Rocchini, D., Marcantonio, M., Ricotta, C., 2017. Measuring Rao's Q diversity index from remote sensing: An open source solution. *Ecol. Indic.* 72, 234–238.
- Rocchini, D., Neteler, M., 2012. Let the four freedoms paradigm apply to ecology. *Trends Ecol. Evol.* 27, 310–311.
- Rocchini, D., Ricotta, C., 2007. Are landscapes as crisp as we may think? *Ecol. Model.* 204, 535–539.
- Rocchini, D., Thouverai, E., Marcantonio, M., Iannacito, M., Re, D.Da., Torresani, M., et al., 2021b. Rasterdiv - An information theory tailored R package for measuring ecosystem heterogeneity from space: To the origin and back. *Methods Ecol. Evol.* 12, 1093–1102.
- Rugani, B., Rocchini, D., 2016. Positioning of remotely sensed spectral heterogeneity in the framework of life cycle impact assessment on biodiversity. *Ecol. Indic.* 61, 923–927.
- Saravia, L.A., 2015. A new method to analyse species abundances in space using generalized dimensions. *Methods Ecol. Evol.* 6, 1298–1310.
- Schneider, F.D., Morsdorf, F., Schmid, B., Petchey, O.L., Hueni, A., Schimel, D.S., Schaeppman, M.E., 2017. Mapping functional diversity from remotely sensed morphological and physiological forest traits. *Nat. Commun.* 1441.
- Shannon, C.E., 1948. A mathematical theory of communication. *Bell Syst. Tech. J.* 27, 379–423.
- Simpson, E.H., 1949. Measurement of diversity. *Nature* 163, 688.
- Skidmore, A.K., Coops, N.C., Neinavaz, E., Alii, A., Schaeppman, M.E., Paganini, M., Kissling, W.D., Vihervaara, P., Darvishzadeh, R., Feilhauer, H., Fernandez, M., Fernandez, N., Gorelick, N., Geizendorfer, I., Heiden, U., Heurich, M., Hobern, D., Holzwarth, S., Muller-Karger, F.E., Van De Kerchove, R., Lausch, A., Leitao, P.J., Lock, M., Mucher, C.A., O'Connor, B., Rocchini, D., Turner, W., Vis, J.-K., Wang, T., Wegmann, M., Wingate, V., 2021. Priority list of biodiversity metrics to observe from space. *Nat. Ecol. Evol.* 5, 896–906.
- Stein, A., Gerstner, K., Kreft, H., 2014. Environmental heterogeneity as a universal driver of species richness across taxa, biomes and spatial scales. *Ecol. Lett.* 17, 866–880.
- Tews, J., Brose, U., Grimm, V., Tielbörger, K., Wichmann, M., Schwager, M., Jeltsch, F., 2004. Animal species diversity driven by habitat heterogeneity/diversity: The importance of keystone structures. *J. Biogeogr.* 31, 79–92.
- Thouverai, E., Marcantonio, M., Bacaro, G., Da Re, D., Iannacito, M., Marchetto, E., Ricotta, C., et al., 2021. Measuring diversity from space: A global view of the free and open source rasterdiv R package under a coding perspective. *Community Ecol.* 22, 1–11.
- Torresani, M., Rocchini, D., Zebisch, M., Sonnenschein, R., Marcantonio, M., Ricotta, C., Tonon, G., 2019. Estimating tree species diversity from space in an alpine conifer forest: The Rao's Q diversity index meets the spectral variation hypothesis. *Ecol. Inform.* 52, 26–34.